MOLECULAR METABOLISM

Dorsolateral septum GLP-1R neurons regulate feeding via lateral hypothalamic projections

Yi Lu[1], Le Wang[1], Fang Luo[1], Rohan Savani[1], Mark A. Rossi[1,2,3,4,*], Zhiping P. Pang[1,4,**]

ABSTRACT

Objective: Although glucagon-like peptide 1 (GLP-1) is known to regulate feeding, the central mechanisms contributing to this function remain enigmatic. Here, we aim to test the role of neurons expressing GLP-1 receptors (GLP-1R) in the dorsolateral septum (dLS; dLS^{GLP-1R}) that project to the lateral hypothalamic area (LHA) on food intake and determine the relationship with feeding regulation.

Methods: Using chemogenetic manipulations, we assessed how activation or inhibition of dLS^{GLP-1R} neurons affected food intake in *Glp1r-ires-Cre* mice. Then, we used channelrhodopsin-assisted circuit mapping, chemogenetics, and electrophysiological recordings to identify and assess the role of the pathway from $dLS^{GLP-1R} \rightarrow$ LHA projections in regulating food intake.

Results: Chemogenetic inhibition of dLS^{GLP-1R} neurons increases food intake. LHA is a major downstream target of dLS^{GLP-1R} neurons. The $dLS^{GLP-1R} \rightarrow$ LHA projections are GABAergic, and chemogenetic inhibition of this pathway also promotes food intake. While chemogenetic activation of $dLS^{GLP-1R} \rightarrow$ LHA projections modestly decreases food intake, optogenetic stimulation of the $dLS^{GLP-1R} \rightarrow$ LHA projection terminals in the LHA rapidly suppresses feeding behavior. Finally, we demonstrate that the GLP-1R agonist, Exendin 4 enhances $dLS^{GLP-1R} \rightarrow$ LHA GABA release.

Conclusions: Together, these results demonstrate that dLS-GLP-1R neurons and the inhibitory pathway to LHA can regulate feeding behavior, which might serve as a potential therapeutic target for the treatment of eating disorders or obesity.

1. INTRODUCTION

Feeding behavior, a highly evolutionarily conserved process critical for survival, is orchestrated by multiple brain regions and related neural circuits in response to external cues and peripheral signals [1—3]. Abnormal activity within feeding circuits may lead to imbalanced food intake and energy expenditure, which can induce changes in body fat mass that can cause obesity and metabolic diseases [1]. However, the neural circuit mechanisms controlling feeding behavior and how their dysfunction leads to disease remain poorly characterized.

Glucagon-like peptide 1 (GLP-1) is an incretin hormone and a post-translational cleavage product of preproglucagon encoded by the pro-glucagon *Gcg* gene, which is primarily produced in the L-cells of the intestine and a subpopulation of hindbrain nucleus tractus solitarius (NTS) neurons [4—7]. GLP-1 actions are mediated by the GLP-1 receptor (GLP-1R), a class B subfamily G protein couple receptor widely expressed in central and peripheral nervous systems [8—10]. Emerging evidence shows that endogenous GLP-1 signaling in both central and peripheral organs can regulate energy homeostasis, including food intake and glucose metabolism [11]. GLP-1 analogs have been used to

treat type 2 diabetes [12], and GLP-1R agonists, such as liraglutide, have recently been approved to treat obesity [11]. Although GLP-1R is widely expressed in brain, the physiological role of GLP-1R neurons in mediating food intake and body weight remains elusive.

One brain region that strongly expresses GLP-1R is the dorsolateral septum (dLS) [13,14], a subcortical forebrain area that exerts influences over feeding behavior [15—18], sleep [19], learning and memory [20—22], mood and motivation [23,24]. Previous studies have suggested GLP-1 acts in the lateral septum to control feeding. For example, infusions of GLP-1 into lateral septum can reduce food intake [25]; however, the involved cell types and neural circuits remain uncharacterized. The LHA has historically been considered a feeding control center that can serve to promote food seeking and intake [26,27]. Emerging evidence showed that the lateral hypothalamic area (LHA) contains functionally opposing neuronal populations that induce diverse feeding behaviors [28,29]. The projections from the septal area to the LHA are implicated in feeding behavioral regulation [30,31], but whether dLS^{GLP-1R} neurons are involved in this pathway remains unknown.

In this study, we sought to determine the role of dLS^{GLP-1R} neurons that project to the LHA in the regulation of food intake. We found that

[1]Child Health Institute of New Jersey, Rutgers Robert Wood Johnson Medical School, New Brunswick, NJ 08901, USA [2]Department of Psychiatry, Rutgers Robert Wood Johnson Medical School, New Brunswick, NJ 08901, USA [3]Brain Health Institute, Rutgers University, New Brunswick, NJ 08901, USA [4]Department of Neuroscience and Cell Biology, Rutgers Robert Wood Johnson Medical School, New Brunswick, NJ 08901, USA

*Corresponding author. Child Health Institute of New Jersey, 89 French Street, Room 3276, New Brunswick, NJ 08901, USA. E-mail: Mark.Rossi@rutgers.edu (M.A. Rossi).

**Corresponding author. Child Health Institute of New Jersey, 89 French Street, Room 3277, New Brunswick, NJ 08901, USA. E-mail: Zhiping.Pang@rutgers.edu (Z.P. Pang).

Original article

chemogenetic inhibition of dLS^{GLP-1R} neurons increased food intake whereas chemogenetic activation of these neurons had no significant effect on feeding, likely due to local inhibition within dLS. Using channelrhodopsin-assisted circuit mapping, we show that a subset of dLS^{GLP-1R} neurons provide functional inhibitory connections onto neurons in LHA. Acute manipulations of this pathway bidirectionally modulate food intake. Collectively, our data demonstrate the role of dLS^{GLP-1R} neurons and their projections to LHA on septo-hypothalamic appetite regulation, providing insights into the central control of feeding behavior.

2. METHOD & MATERIALS

2.1. Animals

All procedures involving mice were approved by the Rutgers University Institutional Animal Care and Use Committee and performed in accordance with the National Institute of Health guidelines for the care and use of laboratory animals. Adult (6—8 weeks old) *Glp1r-ires-Cre* and *Glp1r-ires-Cre:Ai14* male mice were used. Animals were bred in our facility and were maintained at constant temperature (~ 22 °C), humidity (35%—55%), and circadian rhythm (12 h light/dark cycles). Food and water were available in their home cages *ad libitum*.

2.2. Stereotaxic surgery and AAV injections

The AAV-viruses used in this study were purchased from Addgene, include: pAAV-hSyn-DIO-EYFP (Cat. #27056-AAV9), retro-pAAV-Ef1a-DIO-EYFP (Cat. #27056-AAVrg), pAAV-hSyn-fDIO-hM4D(Gi)-mCherry-WPREpA (Cat. #154867-AAV8), pAAV-hSyn-fDIO-hM3D(Gq)-mCherry-WPREpA (Catalog #154868-AAV8), pAAV-Ef1a-fDIO-mCherry (Cat. #114471-AAV8), retro-AAV pEF1a-DIO-FLPo-WPRE-hGHpA (Cat. #87306-AAVrg), pAAV-EF1a-double floxed-hChR2(H134R)-EYFP-WPRE-HGHpA (Cat. #20298-AAV5), AAV-hSyn-DIO-hM4Di-mCherry (Cat. #44362-AAV9), AAV-hSyn-DIO-hM3Dq-mCherry (Cat. #44361-AAV9). Virus expression was allowed for a period of 3 weeks prior to experimental manipulation. For recording CNO-mediated effects of dLS^{GLP-1R} neurons, *Glp1r-ires-Cre* mice were injected bilaterally with either AAV-hSyn-DIO-hM4Di-mCherry or AAV-hSyn-DIO-hM3Dq-mCherry in the dLS allowing identification of dLS^{GLP-1R} neurons for electrophysiological recordings. For Channelrhodopsin-2 (ChR2)-assisted circuit mapping, *Glp1r-ires-Cre* animals were injected with pAAV-EF1a-double floxed-hChR2(H134R)-EYFP into dLS. The injection speed was 1 nL/s while the injection coordinates for dLS were: Anterior-Posterior (AP): +0.5 mm from bregma; Medial-Lateral (ML): ±0.45 mm; Dorsal-Ventral (DV): −2.7 mm. The injection coordinates for the LHA were: AP: −1.2 mm from bregma; ML: ±1 mm; DV: −5.1 mm. Injection sites were confirmed by post hoc histological examinations in all animals reported in this study. 0.1—0.2 μl virus was used for the injection of AAV virus.

2.3. Whole-cell patch clamp electrophysiology in brain slices

Mice were deeply anesthetized with Euthasol and brains were quickly removed into ice-cold oxygenated cutting solution (in mM): 50 sucrose, 2.5 KCl, 0.625 CaCl$_2$, 1.2MgCl$_2$, 1.25NaH$_2$PO$_4$, 25 NaHCO$_3$, and 2.5 glucose saturated with 95% O$_2$/5% CO$_2$. Coronal hypothalamic or dLS slices at 300 μm were prepared using a vibratome (VT 1200 S; Leica). After 1 h recovery (33 °C) in artificial cerebrospinal fluid (ACSF) (in mM): 125 NaCl, 2.5 KCl, 2.5 CaCl$_2$, 1.2 MgCl$_2$, 1.25 NaH$_2$PO$_4$, 25NaHCO$_3$, and 2.5 glucose. Slices were then transferred to a recording chamber and perfused with ACSF recording solution at 30 °C. Patch pipettes (6—9 MΩ) were pulled from borosilicate glass. For current clamp recordings, internal solution contains (in mM): 126 K-gluconate, 4 KCl, 10 HEPES, 4 Mg-ATP, 0.3 Na 2 -GTP, 10 phosphocreatine (pH to 7.2 with KOH); for voltage clamp synaptic recordings, internal solution containing (in mM): 40 CsCl, 90 K-Gluconate, 10 HEPES, 0.05 EGTA, 1.8 NaCl, 3.5 KCl, 1.7 MgCl 2, 2 Mg-ATP, 0.4 Na$_4$-GTP, 10 Phosphocreatine and additional 5 mM QX-314 (pH to 7.2 with CsOH). Whole-cell patch-clamp recordings were performed using an Axon 700B amplifier. Data were filtered at 2 kHz, digitized at 10 kHz and collected using Clampex 10.5 (Molecular Devices).

For chemogenetics recordings, 10 μM Clozapine-N-oxide (CNO) was applied to the bath solution. Neurons exhibiting an increase or decrease in resting membrane potential exceeding 5 mV were considered significantly responsive. For photostimulation (470 nm) -evoked inhibitory post-synaptic currents (IPSCs) recordings, cells were held at −70 mV in the presence of CNQX (20 μM).

2.4. Optical fiber placement

Bilateral optic fibers (RWD, 200 μm diameter core) were implanted into the LHA and fixed to the skull with cement. The coordinates used for the LHA were: AP: −1.2; ML: ±1; DV: −5.1 and AP: −1.2; ML: ±1; DV: −5.0 for the optic fibers. After surgery, mice were housed individually and were allowed to recover for at least 3 weeks before conducting behavioral experiments. The optic fiber location was confirmed by post hoc histological examinations. Data were included only from animals with proper placement.

2.5. Chemogenetics and food intake

Food intake studies on chow were performed as previously described [32]. All animals were singly housed for 3 weeks following surgery and handled for 5 consecutive days before the assay to reduce stress responses. All studies were conducted in a homecage environment with *ad libitum* chow access. A trial consisted of assessing food intake from this study subjects after they received injections of saline or CNO (1 mg/kg i.p.). Saline control experiments were performed with 1 day washout between conditions. CNO tests were conducted with 6 days washout between experiments to ensure the effects of CNO-mediated stimulation had dissipated. Mice with misplaced injections or poor expression were excluded from analysis after post hoc histological examination of mCherry expression. The investigators were blinded to all food intake measurements.

Dark-cycle hM3Dq/hM4Di feeding studies were conducted between 6:00 pm to 9:00 pm (lights off at 6:00 pm) and food intake was monitored 0.5 h, 1 h, 2 h and 3 h starting 30 min after i.p. injection. For post-fast refeed hM3Dq/hM4Di studies, animals were fasted overnight starting at 6:00 pm and food was returned the following morning at 9:00 am. Food intake was monitored 0.5 h, 1 h, 2 h and 3 h after i.p. injection. Light-cycle hM3Dq/hM4Di feeding studies were conducted in *ad libitum* fed mice between 9:00 am to 12:00 pm (lights on at 6:00 am) and food intake was monitored 0.5 h, 1 h, 2 h and 3 h after i.p. injection.

2.6. Optogenetics stimulation and food intake

Optical fibers (200 μm diameter core), NA 0.37 (Thorlabs) were connected the LED generator (473 nm for stimulation, Doric LEDFLP_4ch_1000). A terminal fiber was coupled to a 1.25 OD zirconium ferrule and a mating sleeve which allowed delivery of light to the brain. For in vivo photo-stimulation experiments, 10 ms pulses 1.8 mW 473 nm blue light were given as 25 pulses/s every 1.5 s for 20 min. For the stimulation experiment, animals were provided only 0.5 g food overnight to induce modest food deprivation. All mice were trained for 4 days to acclimate to the feeding schedule before testing. After acclimation, food intake was monitored for 1 h, which consisted of three 20-min blocks: pre-photostimulation, constant

photostimulation, and post-photostimulation. Food intake was measured at 20-, 40-, and 60-min.

2.7. Open field test

Mice were introduced to the middle of a custom-made 45×45 cm square open field arena for 10 min. The mouse's position was tracked from above with a video camera. Mouse position and time spent in the center/peripheral zones were analyzed with custom Python code. The mouse's starting position is defined by the experimenter. Subsequent position is then automatically tracked in each frame by detecting the largest contour and calculating its center of mass. Metrics including the overall distance traversed, duration spent in central versus peripheral areas, and the count of entries into the central zone were calculated. An entry into the center zone was defined as when the center of mass of the animal image enters the center square. Distance traveled and time in center zone were calculated with the custom script. Investigators were blinded to the condition during analysis.

2.8. Light-dark box test

The light–dark box consisting of one dark compartment ($6 \times 5 \times 7$ cm) and one illuminated compartment ($6 \times 5 \times 7$ cm) connected by a door. At the beginning of the experiments, the animals were individually placed into the light compartment facing the dark compartment and then were allowed to freely explore for 5 min. Time spent in the light zone and number of entries into the light zone were measured using SmartCage tracking system (AfaSci).

2.9. Elevated plus maze test

The elevated plus maze consisted of a plus-shaped platform with four intersecting arms: two open arms (30 cm $\times$ 5 cm, wall-free) and two enclosed arms (30 cm $\times$ 5 cm) surrounded by 15-cm-high walls. The maze was elevated 55 cm from the ground. Mice were placed in the center of the apparatus facing an open arm and then allowed to freely explore the maze for 10 min. Light in the open arms was kept at 40 lux. The time spent in the open arm was recorded using a custom Python script designed to automatically detect and track the movement of the animal. Initially, the script captured video input from a USB camera, and the user defined the region of interest (ROI) for both arms of the EPM. The script then identifies the animal's position in each frame by detecting the largest contour and calculating its center of mass. These data were used to track the animal's movement, recording coordinates at each time point. The script then calculated the duration spent in both the open and closed arms along with the number of entries into each arm. An entry was defined as when the center of mass of the animal enters an arm.

2.10. Statistical analysis

Statistical analyses were performed using GraphPad Prism 9. Data were analyzed using Student's two-tailed t-tests for comparisons between two groups and one-way ANOVA followed by Dunnett's multiple comparisons tests or two-way ANOVA followed by Sidak's multiple comparisons tests for comparisons between 3 or more groups. Data are presented as mean $\pm$ SEM. A p-value <0.05 was considered statistically significant.

3. RESULTS

3.1. Chemogenetic inhibition of dLS^{GLP-1R} increases food intake

To examine the role of dLS^{GLP-1R} neurons on food intake, we injected pAAV-hSyn-fDIO-hM4D(Gi)-mCherry in the dLS region of *Glp1r-ires-*

Cre mice to express the inhibitory designer receptors exclusively activated by designer drugs (DREADDs)-hM4Di in dLS^{GLP-1R} neurons (Figure 1A,B). Ex-vivo whole-cell recordings in brain slices confirmed that CNO potently inhibited dLS^{GLP-1R} neurons transduced with the hM4Di. The basal firing rate was reduced, and membrane potentials became more hyperpolarized following CNO application in acute brain slices (Figure 1C). To establish whether these neurons regulate food intake, we measured food intake after chemogenetic inhibition with intraperitoneal (i.p.) administration of CNO (1 mg/kg). We first measured *ad libitum* food intake during the dark and light cycles and found that food intake was significantly increased after chemogenetic inhibition (Figure 1D,E). We also tested this after fasting. Again, we observed that animals with chemogenetic inhibition of dLS^{GLP-1R} neurons ate more food than controls (Figure 1F). These experiments indicate that dLS^{GLP-1R} neurons are involved in food intake regulation.

3.2. Activation of dLS^{GLP-1R} neurons has no significant effect on food intake

Because chemogenetic inhibition of dLS^{GLP-1R} neurons increased food intake, we hypothesized that activation of these neurons would conversely suppress feeding. To test this, we expressed stimulatory Gq-coupled hM3Dq-DREADD in dLS^{GLP-1R} neurons (Figure 2A,B). In contrast to chemogenetic inhibition (Figure 1C), CNO application failed to induce consistent effects on membrane properties in dLS^{GLP-1R} neurons (Figure 2C). After CNO application, 35% (6/17) of neurons showed a hyperpolarized membrane potential and reduced firing rate, whereas 29% (5/17) of neurons showed a depolarized membrane potential and increased firing rate. We then measured food intake after CNO in vivo. Consistent with the varied in vitro recording responses, we did not observe significant effects of CNO administration on food intake in any of the feeding tests (Figure 2D–F). This contradicted our initial hypothesis that activation of dLS^{GLP-1R} neurons would suppress food intake.

We previously demonstrated strong collateral inhibition among dLS neurons [21]. We thus hypothesized that collateral inhibition within dLS may prevent chemogenetic activation from influencing food intake. To test this possibility, we injected Cre-dependent AAVs expressing channelrhodopsin-2 (ChR2) with EYFP into dLS of *Glp1r-ires-Cre* mice and recorded post-synaptic responses from nearby EYFP-negative neurons (Figure 2G). Indeed, light stimulation of ChR2-expressing dLS^{GLP-1R} neurons evoked robust picrotoxin (PTX)-sensitive IPSCs in some neighboring EYFP-negative dLS neurons (6/11) (Figure 2H,I). Taken together, these findings suggest that chemogenetic activation of dLS^{GLP-1R} neurons has no significant effect on food intake, which may be mediated by local inhibition in dLS.

3.3. dLS^{GLP-1R} neurons has no significant impact on stress related behavior

Because previous studies showed that alterations in basal anxiety levels or locomotion may affect feeding behavior [33,34], we investigated whether dLS^{GLP-1R} neural regulation of food intake was secondary to the potential changes in anxiety-like behavior or locomotion. To test this possibility, we performed open-field, light–dark box, and elevated plus maze tests in *Glp1r-ires-Cre* mice transduced with the DREADD-hM3Dq or DREADD-hM4Di in dLS^{GLP-1R} neurons. We observed no changes in basal anxiety-like behavior during chemogenetic inactivation or activation of dLS^{GLP-1R} neurons in these behavioral tests (Fig. S1), suggesting that altered feeding behavior was not induced by changes in basal anxiety levels.
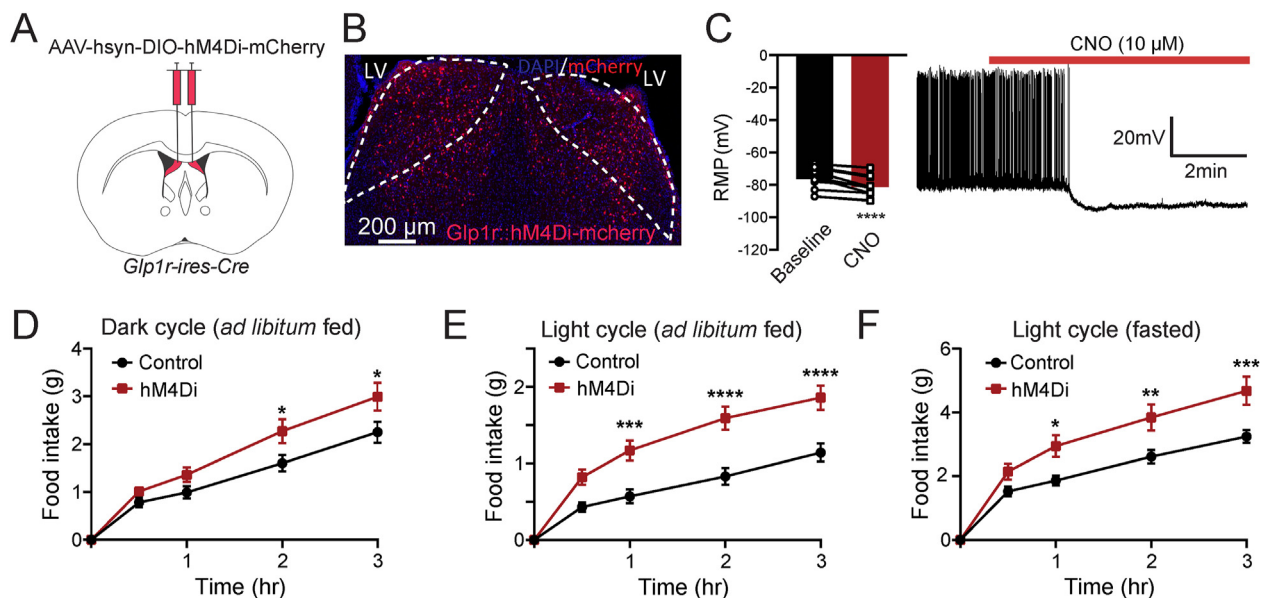
Figure 1: Inhibition of dLS^{GLP-1R} neurons acutely increases food intake.
(A) Brain schematic of viral injection for chemogenetic dLS^{GLP-1R} neurons inhibition.
(B) Transduction of dLS^{GLP-1R} neurons with hM4Di-mCherry.
(C) CNO application hyperpolarized the resting membrane potential and reduced the firing rate of dLS^{GLP-1R} neurons (paired t-test, t(12) = 6.281, p < 0.0001, n = 12 cells from 3 mice).
(D–F) Chemogenetic inhibition of dLS^{GLP-1R} neurons increased food intake (D) during the dark cycle when fed (two-way ANOVA, main effect of Group: F(1,120) = 14.44, p = 0.0002; main effect of time: F(4,120) = 71.72, p < 0.0001, no interaction between Group and Time: F (4,120) = 1.691, p = 0.1566), (E) during the light cycle when fed (two-way ANOVA, main effect of Group: F(1,120) = 53.89, p < 0.0001; main effect of time: F(4,120) = 58.53, p <0.0001, interaction between Group and Time: F(4,120) = 4.284, p = 0.0028) and (F) refeeding following an overnight fast (two-way ANOVA, main effect of Group: F(1,120) = 28.55, p < 0.0001; main effect of Time: F(4,120) = 68.25, p < 0.0001, interaction between Group and Time: F(4,120) = 2.463, p = 0.0488). n = 13 mice per group.
Data are presented as mean ± SEM. Sidak's multiple comparisons test: *p < 0.05; **p < 0.01; ***p < 0.001, ****p < 0.0001.

3.4. dLS^{GLP-1R} neurons project to LHA

Because dLS^{GLP-1R} neuron inhibition increases food intake (Figure 1), we hypothesized that these neurons regulate feeding via long range projections. To determine the downstream targets of dLS^{GLP-1R} neurons, we injected Glp1r-ires-Cre mice in dLS with a Cre-dependent AAV expressing EYFP to visualize axons innervating distal brain regions (Figure 3A). We observed EYFP+ soma in dLS (Figure 3B) and EYFP+ fibers in LHA (Figure 3C), suggesting that dLS^{GLP-1R} neurons send projections to LHA. To further confirm this pathway, we injected a retrograde tracer, retroAAV-Ef1a-DIO-EYFP, in LHA of Glp1r-ires-Cre mice crossed with a Cre-dependent tdTomato reporter line (Ai14) to visualize GLP-1R-expressing neurons (Figure 3D). Unsurprisingly, tdTomato$^+$ cells were distributed evenly throughout the dLS. This expression pattern is consistent with previously published reports [35,36], though we cannot rule out the possibility of sparse expression caused by transient GLP-1R expression during development (thus driving Cre-recombinase expression in these cells). We observed EYFP retrogradely labeled dLS neurons that also expressed tdTomato (Figure 3E,F). Overall, these experiments showed that dLS^{GLP-1R} neurons project to LHA. To further confirm this projection pathways and to reveal the properties of their neurotransmitter release, we performed electrophysiological recordings. In Glp1r-ires-Cre mice we injected Cre-dependent ChR2-EYP in the dLS and made whole cell patch clamp recordings from LHA neurons (Figure 3G). Reliable optogenetic-evoked IPSCs were recorded in LHA neurons (5/8, 62.5%). The blue light-induced PSCs were abolished upon application of TTX and recovered upon application of 4-Aminopyridine (4-AP), suggesting monosynaptic connectivity. Light-evoked PSCs were also abolished

upon application of the GABA$_A$ receptor antagonist picrotoxin (PTX), confirming that dLS^{GLP-1R}→LHA neurons are GABAergic (Figure 3H,I). Taken together, these results show that dLS^{GLP-1R} neurons project to LHA where they form functional inhibitory synapses.

3.5. dLS^{GLP-1R} neurons regulate food intake via projections to LHA

We next asked if dLS^{GLP-1R}→LHA manipulations are sufficient to influence food intake. We used chemogenetic and optogenetic approaches to manipulate dLS^{GLP-1R}→LHA projections and probed their ability to regulate food intake. First, we injected Glp1r-ires-Cre mice with retroAAV-DIO-flp in LHA and AAV-fDIO-hM4Di-mCherry or AAV-fDIO-mCherry in dLS to express the inhibitory DREADDs only in the dLS^{GLP-1R} neurons that project to the LHA (Figure 4A,B). We confirmed the effectiveness of chemogenetic inhibition by in vitro electrophysiology (Figure 4C). Similar to global manipulations of dLS^{GLP-1R} neurons (Figure 1), we observed significant food intake augmentation in inhibiting dLS^{GLP-1R}→LHA neurons (Figure 4D–F), without affecting anxiety-like behaviors (Fig. S2). These data suggest that LHA is likely one of the main targets of dLS^{GLP-1R} neurons that mediates food intake behavior.

Given the possibility that collateral inhibition affects the behavioral expression of activation of dLS^{GLP-1R} neurons (Figure 2), we hypothesized that restricting activation of dLS^{GLP-1R} neurons to those projecting to the LHA would suppress food intake. To test this hypothesis, we injected Glp1r-ires-Cre mice with retroAAV-DIO-flp in LHA and AAV-fDIO-hM3Dq-mCherry or AAV-fDIO-mCherry in dLS to express the excitatory DREADDs in dLS^{GLP-1R}→LHA projections (Figure 5A,B). In contrast to the global dLS^{GLP-1R} activation, we observed consistent
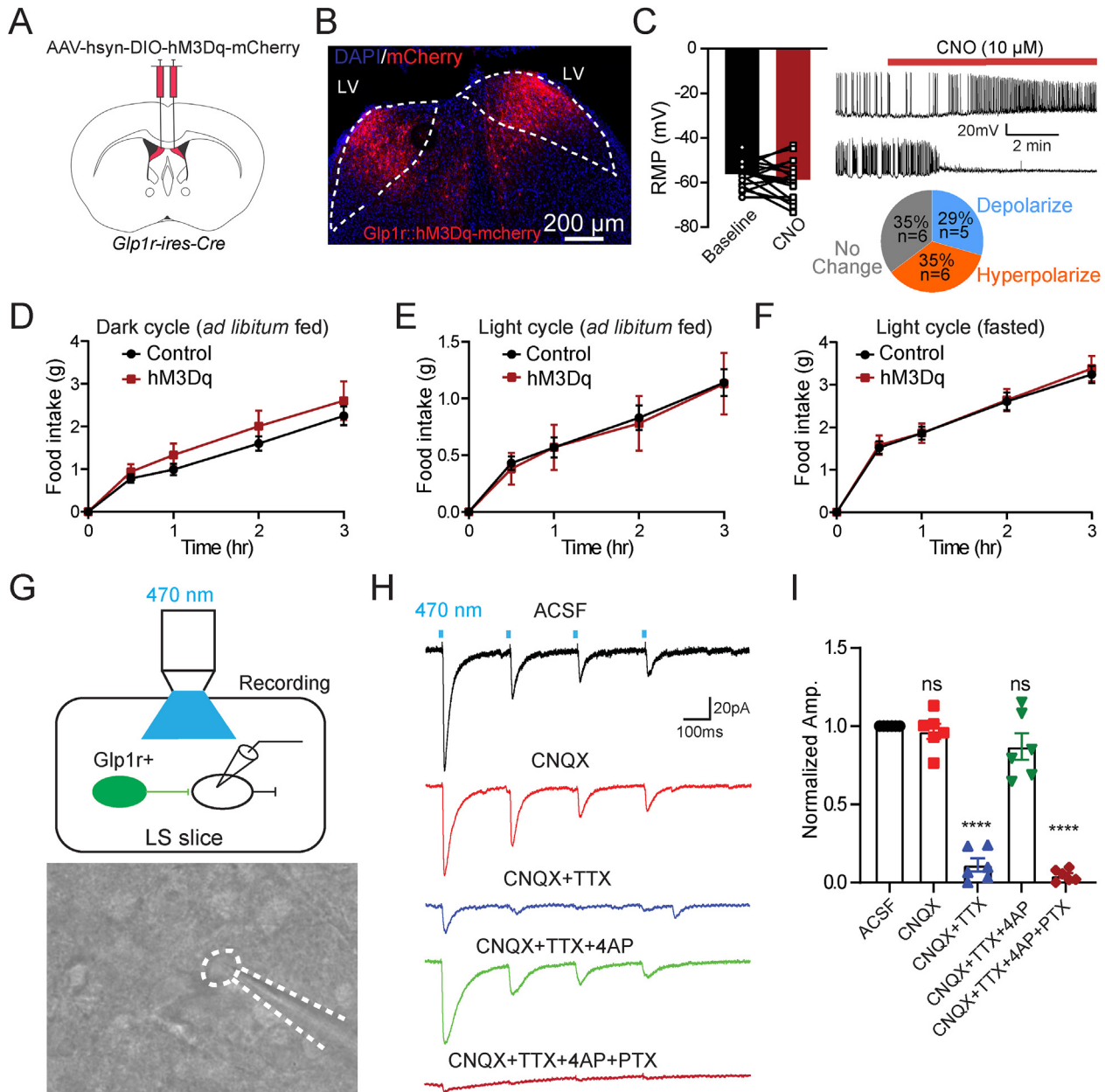
Figure 2: Activation of dLS^{GLP-1R} neurons has no significant effect on food intake.
(A) Brain schematic of viral injection for dLS^{GLP-1R} neuron activation.
(B) Transduction of dLS^{GLP-1R} neurons with hM3Dq-mCherry.
(C) CNO application has no significant effect on the resting membrane potential and the firing rate of dLS^{GLP-1R} neurons (paired t-test, t(17), p = 0.2523, n = 17 cells from 3 mice), after CNO application, 35% of neurons exhibited resting membrane potential hyperpolarization, and 29% of neurons exhibited resting membrane potential depolarization.
(D–F) Chemogenetic activation of dLS^{GLP-1R} neurons has no significant effect on food intake (D) during the dark cycle when fed (two-way ANOVA, no main effect of Group: $F_{(1,105)}$ = 3.402, p = 0.0679; main effect of Time: $F_{(4,105)}$ = 36.10, p < 0.0001, no interaction between Group and Time: $F_{(4,105)}$ = 0.3067, p = 0.8730.), (E) during the light cycle when fed (two-way ANOVA, no main effect of Group: $F_{(1,105)}$ = 0.06226, p = 0.8034; main effect of Time: $F_{(4,105)}$ = 18.67, p < 0.0001, no interaction between Group and Time: $F_{(4,105)}$ = 0.01724, p = 0.9994), and (F) refeeding following an overnight fast (two-way ANOVA, no main effect of Group: $F_{(1,105)}$ = 0.1432, p = 0.7059; main effect of Time: $F_{(4,105)}$ = 84.5, p < 0.0001, no interaction between Group and Time: $F_{(4,105)}$ = 0.04575, p = 0.9960). n = 13 control and 10 hM3Dq mice.
(G–I) Local inhibitory connections in dLS. Schematic showing the experiment used to record postsynaptic currents in local dLS neurons induced by optogenetic stimulation of dLS^{GLP-1R} neurons (G). In brain slice recordings, blue light stimulation evoked robust IPSCs, which were blocked by picrotoxin but not CNQX (H–I) (one-way ANOVA, F (4,25) = 98.81, p < 0.0001, ****Sidak's multiple comparisons test p < 0.0001 vs. ACSF). n = 6 cells from 3 mice.
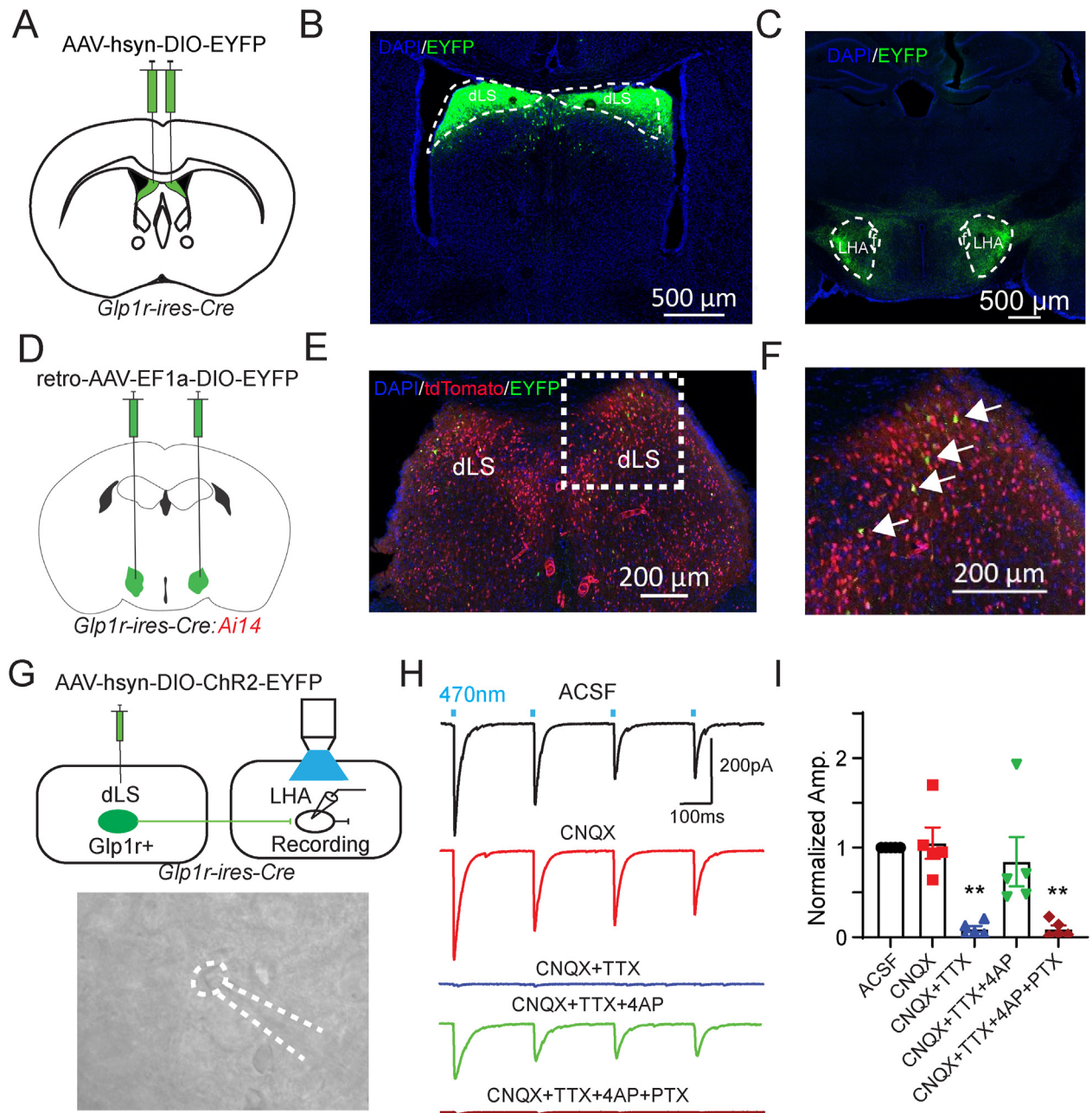Data are presented as mean ± SEM.

Figure 3: dLS^{GLP-1R} neurons project to LHA.

(A) *Glp1r-ires-Cre* mice were injected in dLS with pAAV-hSyn-DIO-EYFP bilaterally.

(B and C) Viral-mediated expression of EYFP in dLS^{GLP-1R} neurons soma (B) and axonal projections in the LHA (C) in *Glp1r-ires-Cre* mice.

(D) *Glp1r-ires-Cre:Ai14* mice were injected in LHA with retro-pAAV-Ef1a-DIO-EYFP bilaterally.

(E and F) Images of coronal brain sections containing the dLS. White arrows indicate GLP-1R+/EYFP+ neurons.

(G) Schematic of experiment used to record postsynaptic currents in LHA neurons induced by optogenetic stimulation of dLS^{GLP-1R} neurons. *Glp1r-ires-Cre* mice were injected in dLS with pAAV-EF1a-double floxed-hChR2(H134R)-EYFP-WPRE-HGHpA bilaterally and LHA neurons were patched.

(H) Representative trace of photostimulation (470 nm LED)-evoked IPSC in LHA neurons, which can be blocked by picrotoxin but not CNQX.

(I) Normalized IPSC amplitude before and after CNQX, TTX, 4AP and PTX application (one-way ANOVA, $F(4,20) = 10.7$, $p < 0.0001$, **Sidak's multiple comparisons test $p < 0.01$ vs. ACSF). n = 5 cells from 3 mice.

Data are presented as mean ± SEM.

membrane depolarization of hM3Dq-expressing neurons when CNO was applied *ex vivo* (Figure 5C). Upon CNO administration in vivo, we observed no change in food intake in either the dark or light cycles when animals were *ad libitum* fed (Figure 5D,E). However, food intake was significantly reduced when animals were tested in the light cycle following fasting (Figure 5F). Anxiety-like behavior was again unchanged in these animals (Fig. S3).

To further probe whether acute activation of the dLS^{GLP-1R}→LHA pathway could suppress feeding, we next performed projection-specific optogenetic stimulation. We expressed Cre-dependent
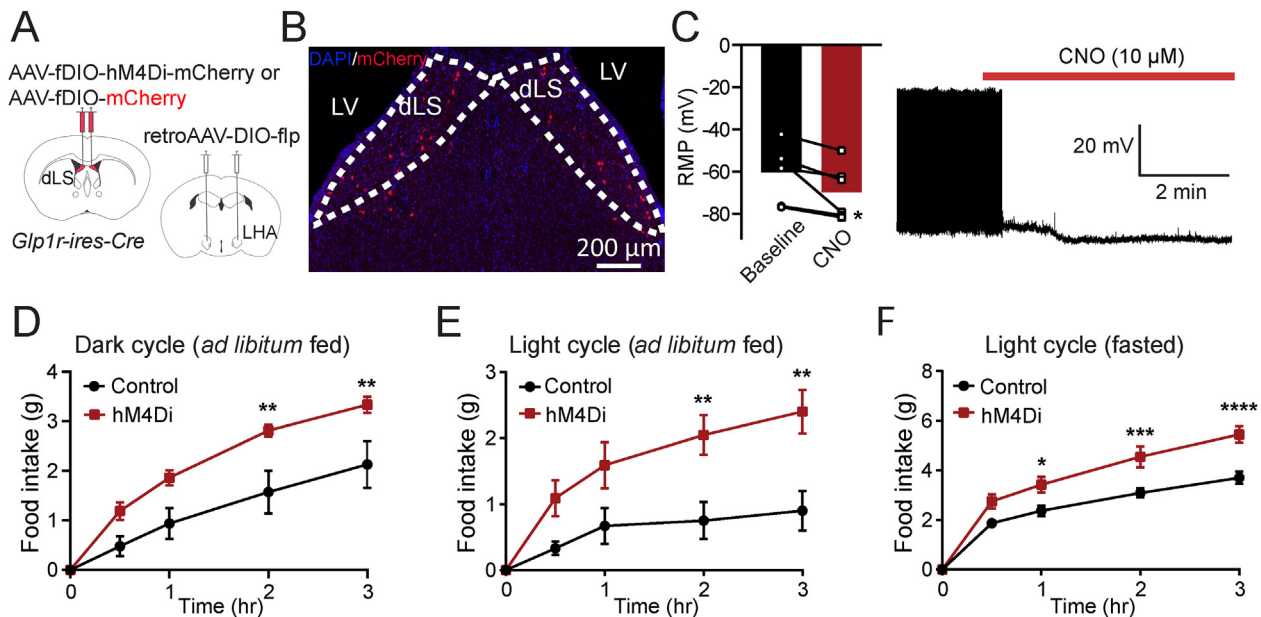
Figure 4: dLS^{GLP-1R} → LHA inhibition increases feeding.
(A) Brain schematic of viral injection for dLS^{GLP-1R} → LHA neuron inhibition.
(B) Transduction of dLS^{GLP-1R} → LHA neurons with hM4Di-mCherry.
(C) CNO application hyperpolarized the resting membrane potential and reduced the firing rate of dLS^{GLP-1R} → LHA projection neurons (paired t-test, t(6) = 2.897, p = 0.0339, n = 6 cells from 3 mice).
(D−F) Chemogenetic inhibition of dLS^{GLP-1R} → LHA projection neurons increased food intake (D) during the dark cycle when fed (two-way ANOVA, main effect of Group: $F_{(1,40)}$ = 26.01, p < 0.0001; main effect of Time: $F_{(4,40)}$ = 36.65, p < 0.0001, no interaction between Group and Time: $F_{(4,40)}$ = 1.993, p = 0.1142), (E) during the light cycle when fed (two-way ANOVA, main effect of Group: $F_{(1,60)}$ = 27.88, p < 0.0001; main effect of Time: $F_{(4,60)}$ = 11.68, p < 0.0001, no interaction between Group and Time: $F_{(4,60)}$ = 2.344, p = 0.0649), and (F) refeeding following an overnight fast (two-way ANOVA, main effect of Group: $F_{(1,55)}$ = 44.88, p < 0.0001; main effect of Time: $F_{(4,55)}$ = 104, p < 0.0001, interaction between Group and Time: $F_{(4,55)}$ = 3.795, p = 0.00085). n = 7 control an d6 hM4Di mice. Sidak's multiple comparisons test: *p < 0.05, **p < 0.01, ***p < 0.001, ****p < 0.0001.
Data are presented as mean ± SEM.

ChR2-EYFP in dLS of *Glp1r-ires-Cre* mice and implanted optical fibers in the LHA to selectively stimulate the dLS^{GLP-1R}→LHA pathways (Figure 6A,B). Indeed, optogenetic activation of dLS^{GLP-1R}→LHA nerve terminals significantly suppressed feeding in fasted mice, which returned to control levels when stimulation ceased (Figure 6C).

Finally, since these dLS^{GLP-1R}→LHA neurons express GLP-1R, we asked if GLP-1R-mediated signaling affects dLS^{GLP-1R}→LHA synaptic strength [37]. We recorded from LHA neurons that receive inhibitory synaptic input from dLS^{GLP-1R} neurons (Figure 6D). Consistent with our hypothesis, optically induced IPSCs in LHA neurons were enhanced by application of the GLP-1R agonist, Exendin 4 (Exn4) (Figure 6E,F). This synaptic augmentation is accompanied by a reduction of paired-pulse ratio (PPR), suggesting the involvement of a presynaptic mechanism.

Overall, these experiments establish that dLS^{GLP-1R} neurons and their inhibitory projections to the LHA regulate food intake independent of changes in basal anxiety levels.

4. DISCUSSION

Our data demonstrate that dLS^{GLP-1R} neuron inhibition potentiates food intake without affecting changes in anxiety-like behavior and locomotion. Previous studies have shown that the projections from the lateral septum to hypothalamic nuclei and the amygdala mediate stress and anxiety-like behavior, including both anxiolytic and anxiogenic effects [38−43]. We found that manipulations of dLS^{GLP-1R} neurons or their projections to the LHA failed to affect anxiety-like

behavior while still influencing food intake. This suggests that this population may be selectively involved in the control of feeding behavior. However, the lack of obvious effects on anxiety-like behavior in this study may be due to the possibility that we manipulated neurons that mediate both anxiolytic and anxiogenic behaviors. Although no consensus exists from controlled trials in humans regarding the ability of GLP-1R agonists to influence mood, emerging evidence suggests that anxiety and stress may be reduced by liraglutide [44,45]. However, dissociating these effects from indirect effects on mood caused by weight loss can be challenging. We therefore speculate that GLP-1R agonists act on diverse neurocircuits where they exert varied behavioral effects based on the specific neurocircuit function. They may act on other descending LS pathways to influence stress and anxiety-like behavior and simultaneously act on other circuits (e.g., the dLS→LHA pathway) to curb appetite.

Consistent with our observations, emerging evidence has demonstrated that the lateral septum contributes to appetite suppression [17,30] and food-seeking behaviors [31]. We extend these findings by demonstrating a selective role of dLS^{GLP-1R} neurons in regulating food intake. In the current study, we show that chemogenetic dLS^{GLP-1R} neuron inhibition increases food intake; however, chemogenetic activation of the same population failed to affect food intake. It has previously been shown that GABAergic neurons comprise more than 90% of all LS neurons [46]. Consistent with our data indicating GABA release, dLS^{GLP-1R} neurons have previously been shown to overlap almost entirely with GABAergic markers [14,36]. We therefore hypothesized that local inhibitory connections within the dLS result in some cells being
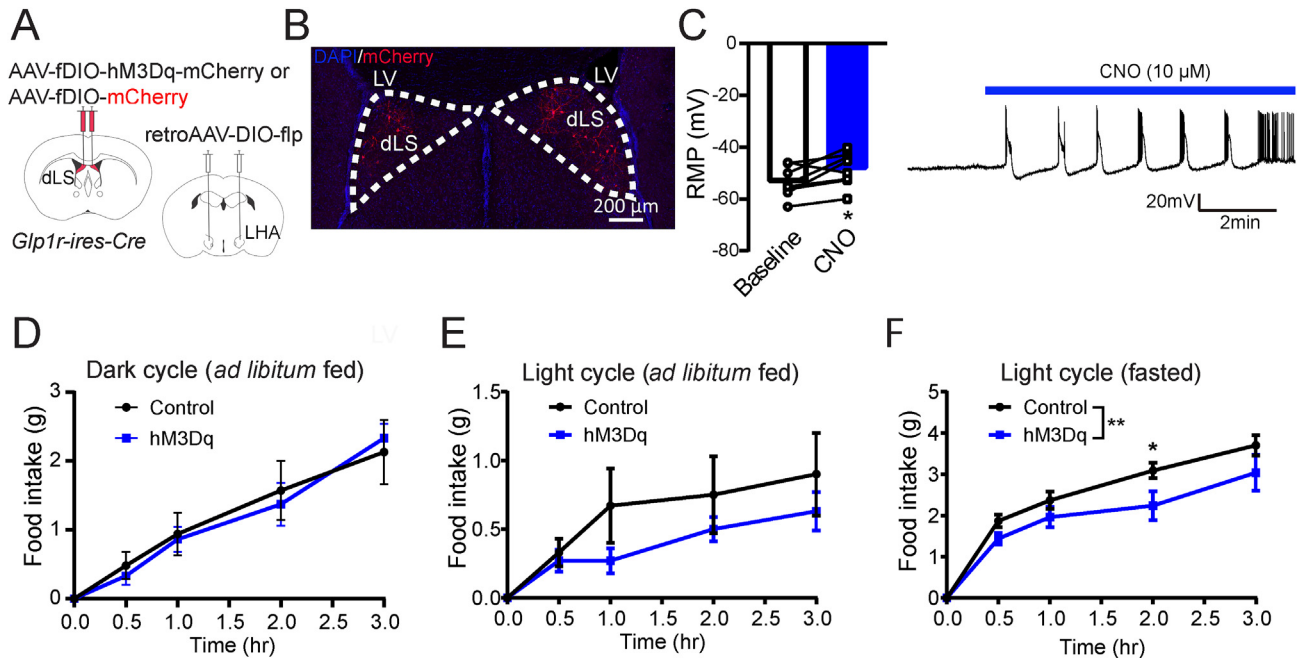
Figure 5: Activation of dLS^{GLP-1R} projection neurons has no significant effect on food intake.
(A) Brain schematic of viral injection for dLS^{GLP-1R} → LHA neuron activation.
(B) Transduction of dLS^{GLP-1R} → LHA neurons with hM3Dq-mCherry.
(C) CNO application depolarized the resting membrane potential and increased the firing rate of dLS^{GLP-1R}→LHA projection neurons (paired t-test, $t(8) = 2.702$, $p = 0.0306$, $n = 8$ cells from 3 mice).
(D–F) Chemogenetic activation of dLS^{GLP-1R} → LHA projection neurons has no significant effect on food intake (D) during the dark cycle when fed (two-way ANOVA, no main effect of Group: $F_{(1,45)} = 0.07858$, $p = 0.7805$; main effect of Time: $F_{(4,45)} = 23.01$, $p < 0.0001$, no interaction between Group and Time: $F_{(4,45)} = 0.1826$, $p = 0.9463$), (E) during the light cycle when fed (two-way ANOVA, a marginally significant main effect of Group: $F_{(1,50)} = 3.272$, $p = 0.0765$; main effect of Time: $F_{(4,50)} = 6.024$, $p = 0.0005$, no interaction between Group and Time: $F_{(4,50)} = 0.4554$, $p = 0.7680$). (F) Chemogenetic activation suppressed food intake during refeeding following an overnight fast (two-way ANOVA, main effect of Group: $F_{(1,50)} = 11.01$, $p = 0.0017$; main effect of Time: $F_{(4,50)} = 64.4$, $p < 0.0001$, no interaction between Group and Time: $F_{(4,50)} = 1.013$, $p = 0.4096$). $n = 7$ control and 5 hM3Dq mice.
Data are presented as mean ± SEM.

inhibited during dLS^{GLP-1R} neuron activation. Using optogenetics-assisted circuit mapping, we indeed recorded GABA release in dLS after GLP-1R neuron activation. In support of this, a previous study showed that activation of LS adenosine A$_{2A}$ receptor-expressing GABAergic neurons suppressed the activity of surrounding LS cells, as concluded by decreased c-Fos-immunoreactivity [47]. Our data demonstrating both depolarization and hyperpolarization of dLS^{GLP-1R} neurons upon chemogenetic activation are consistent with this observation. Although our data are suggestive of collateral inhibition within the dLS and are consistent with published reports [21], we cannot rule out the possibility of more complex circuit-level effects. Future studies will be needed to fully dissect the dLS^{GLP-1R} neuron microcircuitry.

It is well established that the LS is strongly connected with the hypothalamus [48], which critically mediates feeding behavior and energy homeostasis [28]. Within the hypothalamus, the LHA also exerts control over motivated behavior, feeding, and energy balance across species [49]. Here, we found that dLS^{GLP-1R} neurons provide GABAergic input to the LHA. Our data demonstrate that chemogenetic or optogenetic stimulation of dLS^{GLP-1R}→LHA neurons suppresses food intake, whereas chemogenetic inhibition of this pathway increase feeding. These results suggest a feeding-specific pathway from dLS to LHA. The LHA contains many molecularly and functionally distinct cell types [50–53]. Among these, GABAergic LHA neurons promote food seeking, consumption, and positive energy balance [49,54]. We therefore speculate that GABAergic neurons are the downstream target of dLS^{GLP-1R} neurons within the LHA. Our data are consistent with this

possibility because reduced inhibitory tone onto LHA GABA neurons (e.g., during chemogenetic inhibition of dLS^{GLP-1R} neurons) is expected to activate these cells and consequently increase feeding. Consistent with this, it has recently been shown that the anti-obesity drug Tesofensine reduces the activity of LHA GABA neurons [55]. In addition to GABAergic neurons, there are also abundant melanin-concentrating hormone (MCH) and orexin/hypocretin neuron populations in the LHA. Much evidence indicates that these cells can also promote food intake and regulate energy metabolism [56–59]. Therefore, MCH and orexin/hypocretin cells may also be downstream targets of dLS^{GLP-1R}→LHA neurons.

For decades, GLP-1 has been known to reduce food intake by acting as a short-term prandial signal [6]. However, GLP-1 is also produced in the brain and is involved in a satiation/satiety circuit controlling food intake and body weight [37,60,61]. GLP-1 actions are mediated by GLP-1R, which is widely expressed in both the periphery [62] and the brain, including the dLS, LHA, and paraventricular hypothalamic nucleus, among other regions. GLP-1R agonists, such as the analog of GLP-1 (liraglutide), have been used clinically as therapies to combat obesity [11]. Previous studies have shown that endogenous activation of LS GLP-1R plays a role in feeding in both rats and mice [13,63]. However, the source of endogenous GLP-1 within the dLS^{GLP-1R}→LHA pathway is not yet known. It has recently been shown that the GLP-1R agonist liraglutide is transported into the brain via tanycytes [64]. This can provide direct access of liraglutide to the hypothalamus. Similarly, Exn4, another GLP-1R agonist, has been shown to cross the blood brain barrier
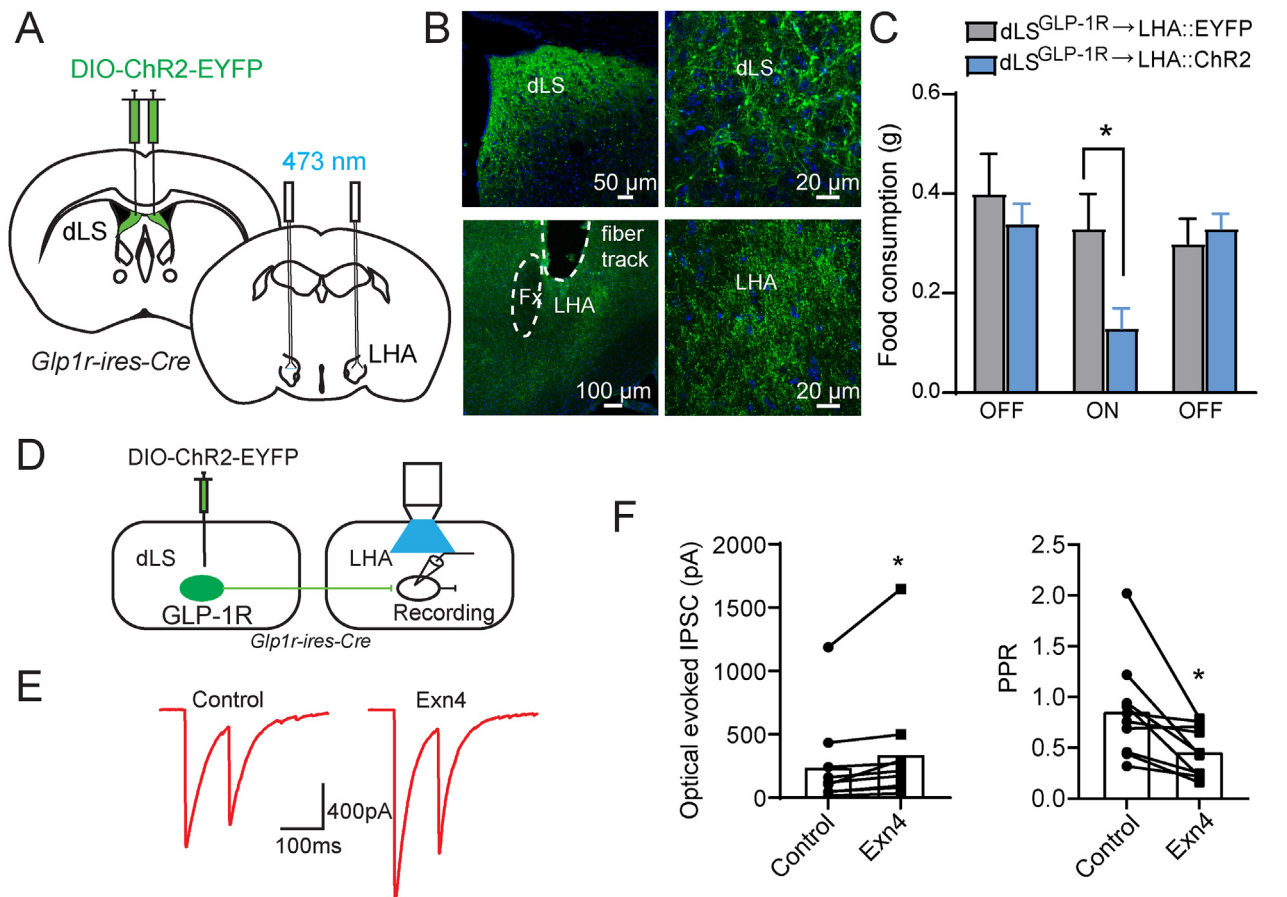
Figure 6: dLS^{GLP-1R}→LHA activation suppresses feeding.
(A and B) ChR2-EYFP expression in the dLS (A) and axonal projections in the LHA (B) in *Glp1r-ires-Cre* mice.
(C) Photostimulation of dLS^{GLP-1R} → LHA projections significantly suppressed food intake (two-way ANOVA, main effect of Group: $F_{(1,36)}$ = 3.382, p = 0.0742; main effect of Stimulation: $F_{(2,36)}$ = 3.816, p = 0.0314, no interaction between Group and Stimulation: $F_{(2,36)}$ = 2.576, p = 0.0900. *Sidak's multiple comparisons test $p < 0.05$. Data are presented as mean + SEM. n = 6 controls and 8 ChR2 mice.
(D) Experimental paradigm for recording postsynaptic currents in LHA slices induced by optogenetic stimulation of dLS^{GLP-1R} neurons.
(E) Representative evoked IPSCs after paired-pulse optogenetic stimulation.
(F) Quantification of evoked IPSCs (paired t-test, $t_{(10)}$ = 2.312, p = 0.0461) and PPR (paired t-test, $t_{(10)}$ = 3.135, p = 0.0120) before and after Exn4 application. n = 10 cells from 3 mice. *$p < 0.05$.

[65]; however, it is unknown if peripherally administered GLP-1R agonists can reach the dLS [66]. An additional possibility is that GLP-1 reaches the dLS and LHA via an ascending central pathway. For example, GLP-1 neurons reside within the NTS and have been shown to send projections to the septal area [67,68], but whether this pathway is the sole source of LS GLP-1 is unclear. Thus, the source(s) of endogenous dLS GLP-1 as well as whether current therapeutics exert appetite suppressing effects via the dLS remain to be determined.

In this study, we also find that Exn4 can increase the optically induced IPSCs and increase the presynaptic release probability at the dLS^{GLP-1R}→LHA synapse, suggesting that GLP-1 signaling may mediate this pathway's influence on feeding behavior. Our results indicate that Exn4 acts on presynaptic GLP-1Rs within the LHA. Given the observation that Exn4 also acts on GLP-1Rs within the LS to suppress food intake [25], our results suggest that drugs targeting GLP-1R can act at both the soma and synapse within this pathway. We speculate that agonizing GLP-1Rs with Exn4 would occlude or attenuate the effects of dLS^{GLP-1R} and dLS^{GLP-1R}→LHA neuron inhibition on food intake. However, it is unlikely that Exn4 application would completely prevent feeding elicited by dLS^{GLP-1R} neuron inhibition

because these effects are likely mediated primarily by GABA. Nevertheless, this may be difficult to elucidate because of the profound impact of GLP-1 agonists on feeding, and basal levels of feeding during such pharmacological interventions are already quite low. Moreover, Exn4 is also known to act outside the dLS→LHA pathway to reduce appetite [69]. Future studies will be required to determine the specific contributions of dLS$^{GLP-1Rs}$ to feeding behavior.

In this study, we found that dLS^{GLP-1R} neurons and their inhibitory projections to the LHA can bidirectionally regulate food intake. These results extend our understanding of the neural mechanisms underlying feeding behavior and energy homeostasis. However, important unresolved questions remain. We have found local inhibitory connections within the dLS, which may have complex circuit architecture. For this reason, the specific mechanisms and functions of this local inhibition remain unclear. Our data demonstrate that Exn4 can augment the optically evoked IPSCs likely via increasing the presynaptic release probability at the dLS^{GLP-1R}→LHA synapse. Behavioral evidence on systematic pharmacological application of GLP-1R and specific neural circuits, including the dLS^{GLP-1R} → LHA, should be conducted in future studies. Moreover, while we speculate that the downstream target of

Original article

dLS^{GLP-1R}→LHA neurons are GABAergic neurons, further studies are required to elucidate these details.

5. CONCLUSIONS

Here, we dissected the role of dLS^{GLP-1R} neurons and their projections to the LHA in regulating feeding behavior. We showed that manipulations of both dLS^{GLP-1R} neurons or their projections to the LHA can influence feeding behavior independent of changes to anxiety-like behavior. A subpopulation of dLS^{GLP-1R} neurons send monosynaptic projections to the LHA where they release GABA, and the strength of this synapse is enhanced by GLP-1 signaling.

CREDIT AUTHORSHIP CONTRIBUTION STATEMENT

Yi Lu: Writing — review & editing, Writing — original draft, Visualization, Investigation, Formal analysis, Conceptualization. **Le Wang:** Writing — review & editing, Investigation. **Fang Luo:** Investigation. **Rohan Savani:** Writing — review & editing, Investigation. **Mark A. Rossi:** Writing — review & editing, Writing — original draft, Supervision, Investigation, Funding acquisition. **Zhiping P. Pang:** Writing — review & editing, Writing — original draft, Supervision, Investigation, Funding acquisition, Conceptualization.

DECLARATION OF COMPETING INTEREST

The authors declare that they have no known competing financial interests or personal relationships that could have appeared to influence the work reported in this paper.

DATA AVAILABILITY

Data will be made available on request.

APPENDIX A. SUPPLEMENTARY DATA

Supplementary data to this article can be found online at https://doi.org/10.1016/j.molmet.2024.101960.

REFERENCES

[1] Morton GJ, Meek TH, Schwartz MW. Neurobiology of food intake in health and disease. Nat Rev Neurosci 2014;15(6):367—78.

[2] Rossi MA, Stuber GD. Overlapping brain circuits for homeostatic and hedonic feeding. Cell Metabol 2018;27(1):42—56.

[3] Sohn JW, Elmquist JK, Williams KW. Neuronal circuits that regulate feeding behavior and metabolism. Trends Neurosci 2013;36(9):504—12.

[4] Drucker DJ. Mechanisms of action and therapeutic application of glucagon-like peptide-1. Cell Metabol 2018;27(4):740—56.

[5] Muller TD, Finan B, Bloom SR, D'Alessio D, Drucker DJ, Flatt PR, et al. Glucagon-like peptide 1 (GLP-1). Mol Metabol 2019;30:72—130.

[6] Holst JJ. The physiology of glucagon-like peptide 1. Physiol Rev 2007;87(4): 1409—39.

[7] Larsen PJ, Tang-Christensen M, Holst JJ, Orskov C. Distribution of glucagon-like peptide-1 and other preproglucagon-derived peptides in the rat hypothalamus and brainstem. Neuroscience 1997;77(1):257—70.

[8] McLean BA, Wong CK, Campbell JE, Hodson DJ, Trapp S, Drucker DJ. Revisiting the complexity of GLP-1 action from sites of synthesis to receptor activation. Endocr Rev 2021;42(2):101—32.

[9] Gromada J, Holst JJ, Rorsman P. Cellular regulation of islet hormone secretion by the incretin hormone glucagon-like peptide 1. Pflügers Archiv 1998;435(5): 583—94.

[10] Sandoval D. CNS GLP-1 regulation of peripheral glucose homeostasis. Physiol Behav 2008;94(5):670—4.

[11] Drucker DJ. GLP-1 physiology informs the pharmacotherapy of obesity. Mol Metabol 2022;57:101351.

[12] Lovshin JA, Drucker DJ. Incretin-based therapies for type 2 diabetes mellitus. Nat Rev Endocrinol 2009;5(5):262—9.

[13] Terrill SJ, Holt MK, Maske CB, Abrams N, Reimann F, Trapp S, et al. Endogenous GLP-1 in lateral septum promotes satiety and suppresses motivation for food in mice. Physiol Behav 2019;206:191—9.

[14] Harasta AE, Power JM, von Jonquieres G, Karl T, Drucker DJ, Housley GD, et al. Septal glucagon-like peptide 1 receptor expression determines suppression of cocaine-induced behavior. Neuropsychopharmacology 2015;40(8): 1969—78.

[15] Scopinho AA, Resstel LB, Correa FM. alpha(1)-Adrenoceptors in the lateral septal area modulate food intake behaviour in rats. Br J Pharmacol 2008;155(5):752—6.

[16] Mitra A, Lenglos C, Timofeeva E. Activation of GABAA and GABAB receptors in the lateral septum increases sucrose intake by differential stimulation of sucrose licking activity. Behav Brain Res 2014;273:82—8.

[17] Sweeney P, Yang Y. An excitatory ventral hippocampus to lateral septum circuit that suppresses feeding. Nat Commun 2015;6:10188.

[18] Urstadt KR, Stanley BG. Direct hypothalamic and indirect trans-pallidal, trans-thalamic, or trans-septal control of accumbens signaling and their roles in food intake. Front Syst Neurosci 2015;9:8.

[19] Wang D, Guo Q, Zhou Y, Xu Z, Hu SW, Kong XX, et al. GABAergic neurons in the dorsal-intermediate lateral septum regulate sleep-wakefulness and anesthesia in mice. Anesthesiology 2021;135(3):463—81.

[20] Tingley D, Buzsaki G. Transformation of a spatial map across the hippocampal-lateral septal circuit. Neuron 2018;98(6):1229—42. e1225.

[21] Liu JJ, Tsien RW, Pang ZP. Hypothalamic melanin-concentrating hormone regulates hippocampus-dorsolateral septum activity. Nat Neurosci 2022;25(1):61—71.

[22] Besnard A, Miller SM, Sahay A. Distinct dorsal and ventral hippocampal CA3 outputs govern contextual fear discrimination. Cell Rep 2020;30(7):2360—73. e2365.

[23] Wirtshafter HS, Wilson MA. Lateral septum as a nexus for mood, motivation, and movement. Neurosci Biobehav Rev 2021;126:544—59.

[24] Sheehan TP, Chambers RA, Russell DS. Regulation of affect by the lateral septum: implications for neuropsychiatry. Brain Res Brain Res Rev 2004;46(1): 71—117.

[25] Terrill SJ, Jackson CM, Greene HE, Lilly N, Maske CB, Vallejo S, et al. Role of lateral septum glucagon-like peptide 1 receptors in food intake. Am J Physiol Regul Integr Comp Physiol 2016;311(1):R124—32.

[26] Margules DL, Olds J. Identical "feeding" and "rewarding" systems in the lateral hypothalamus of rats. Science 1962;135(3501):374—5.

[27] Anand BK, Brobeck JR. Localization of a "feeding center" in the hypothalamus of the rat. Proc Soc Exp Biol Med 1951;77(2):323—4.

[28] Stuber GD, Wise RA. Lateral hypothalamic circuits for feeding and reward. Nat Neurosci 2016;19(2):198—205.

[29] Berthoud HR, Munzberg H. The lateral hypothalamus as integrator of metabolic and environmental needs: from electrical self-stimulation to opto-genetics. Physiol Behav 2011;104(1):29—39.

[30] Sweeney P, Yang Y. An inhibitory septum to lateral hypothalamus circuit that suppresses feeding. J Neurosci 2016;36(44):11185—95.

[31] Carus-Cadavieco M, Gorbati M, Ye L, Bender F, van der Veldt S, Kosse C, et al. Gamma oscillations organize top-down signalling to hypothalamus and enable food seeking. Nature 2017;542(7640):232—6.

[32] Li C, Navarrete J, Liang-Guallpa J, Lu C, Funderburk SC, Chang RB, et al. Defined paraventricular hypothalamic populations exhibit differential responses to food contingent on caloric state. Cell Metab 2019;29(3):681—94. e685.

[33] Azevedo EP, Tan B, Pomeranz LE, Ivan V, Fetcho R, Schneeberger M, et al. A limbic circuit selectively links active escape to food suppression. Elife 2020;9.

[34] Xu Y, Lu Y, Cassidy RM, Mangieri LR, Zhu C, Huang X, et al. Identification of a neurocircuit underlying regulation of feeding by stress-related emotional responses. Nat Commun 2019;10(1):3446.

[35] Cork SC, Richards JE, Holt MK, Gribble FM, Reimann F, Trapp S. Distribution and characterisation of Glucagon-like peptide-1 receptor expressing cells in the mouse brain. Mol Metab 2015;4(10):718—31.

[36] Graham DL, Durai HH, Trammell TS, Noble BL, Mortlock DP, Galli A, et al. A novel mouse model of glucagon-like peptide-1 receptor expression: a look at the brain. J Comp Neurol 2020;528(14):2445—70.

[37] Liu J, Conde K, Zhang P, Lilascharoen V, Xu Z, Lim BK, et al. Enhanced AMPA receptor trafficking mediates the anorexigenic effect of endogenous glucagon-like peptide-1 in the paraventricular hypothalamus. Neuron 2017;96(4):897—909. e895.

[38] Bakshi VP, Newman SM, Smith-Roe S, Jochman KA, Kalin NH. Stimulation of lateral septum CRF2 receptors promotes anorexia and stress-like behaviors: functional homology to CRF1 receptors in basolateral amygdala. J Neurosci 2007;27(39):10568—77.

[39] Singewald GM, Rjabokon A, Singewald N, Ebner K. The modulatory role of the lateral septum on neuroendocrine and behavioral stress responses. Neuropsychopharmacology 2011;36(4):793—804.

[40] Anthony TE, Dee N, Bernard A, Lerchner W, Heintz N, Anderson DJ. Control of stress-induced persistent anxiety by an extra-amygdala septohypothalamic circuit. Cell 2014;156(3):522—36.

[41] Mitra A, Lenglos C, Timofeeva E. Inhibition in the lateral septum increases sucrose intake and decreases anorectic effects of stress. Eur J Neurosci 2015;41(4):420—33.

[42] Wang D, Pan X, Zhou Y, Wu Z, Ren K, Liu H, et al. Lateral septum-lateral hypothalamus circuit dysfunction in comorbid pain and anxiety. Mol Psychiatr 2023;28(3):1090—100.

[43] Patel H. The role of the lateral septum in neuropsychiatric disease. J Neurosci Res 2022;100(7):1422—37.

[44] Bode BW, Testa MA, Magwire M, Hale PM, Hammer M, Blonde L, et al. Patient-reported outcomes following treatment with the human GLP-1 analogue liraglutide or glimepiride in monotherapy: results from a randomized controlled trial in patients with type 2 diabetes. Diabetes Obes Metabol 2010;12(7):604—12.

[45] Tsai WH, Sung FC, Chiu LT, Shih YH, Tsai MC, Wu SI. Decreased risk of anxiety in diabetic patients receiving glucagon-like peptide-1 receptor agonist: a nationwide, population-based cohort study. Front Pharmacol 2022;13:765446.

[46] Zhao C, Eisinger B, Gammie SC. Characterization of GABAergic neurons in the mouse lateral septum: a double fluorescence in situ hybridization and immunohistochemical study using tyramide signal amplification. PLoS One 2013;8(8):e73750.

[47] Wang M, Li P, Li Z, da Silva BS, Zheng W, Xiang Z, et al. Lateral septum adenosine A(2A) receptors control stress-induced depressive-like behaviors via signaling to the hypothalamus and habenula. Nat Commun 2023;14(1):1880.

[48] Risold PY, Swanson LW. Connections of the rat lateral septal complex. Brain Res Brain Res Rev 1997;24(2—3):115—95.

[49] Rossi MA. Control of energy homeostasis by the lateral hypothalamic area. Trends Neurosci 2023;46(9):738—49.

[50] Rossi MA, Basiri ML, McHenry JA, Kosyk O, Otis JM, van den Munkhof HE, et al. Obesity remodels activity and transcriptional state of a lateral hypothalamic brake on feeding. Science 2019;364(6447):1271—4.

[51] Mickelsen LE, Bolisetty M, Chimileski BR, Fujita A, Beltrami EJ, Costanzo JT, et al. Single-cell transcriptomic analysis of the lateral hypothalamic area reveals molecularly distinct populations of inhibitory and excitatory neurons. Nat Neurosci 2019;22(4):642—56.

[52] Rossi MA, Basiri ML, Liu Y, Hashikawa Y, Hashikawa K, Fenno LE, et al. Transcriptional and functional divergence in lateral hypothalamic glutamate neurons projecting to the lateral habenula and ventral tegmental area. Neuron 2021;109(23):3823—37. e3826.

[53] Wang Y, Eddison M, Fleishman G, Weigert M, Xu S, Wang T, et al. EASI-FISH for thick tissue defines lateral hypothalamus spatio-molecular organization. Cell 2021;184(26):6361—77. e6324.

[54] Jennings JH, Ung RL, Resendez SL, Stamatakis AM, Taylor JG, Huang J, et al. Visualizing hypothalamic network dynamics for appetitive and consummatory behaviors. Cell 2015;160(3):516—27.

[55] Perez CI, Luis-Islas J, Lopez A, Diaz X, Molina O, Arroyo B, et al. Tesofensine, a novel antiobesity drug, silences GABAergic hypothalamic neurons. PLoS One 2024;19(4):e0300544.

[56] Pissios P, Bradley RL, Maratos-Flier E. Expanding the scales: the multiple roles of MCH in regulating energy balance and other biological functions. Endocr Rev 2006;27(6):606—20.

[57] Al-Massadi O, Dieguez C, Schneeberger M, Lopez M, Schwaninger M, Prevot V, et al. Multifaceted actions of melanin-concentrating hormone on mammalian energy homeostasis. Nat Rev Endocrinol 2021;17(12):745—55.

[58] Lord MN, Subramanian K, Kanoski SE, Noble EE. Melanin-concentrating hormone and food intake control: sites of action, peptide interactions, and appetition. Peptides 2021;137:170476.

[59] Bouaouda H, Jha PK. Orexin and MCH neurons: regulators of sleep and metabolism. Front Neurosci 2023;17:1230428.

[60] Baggio LL, Drucker DJ. Glucagon-like peptide-1 receptors in the brain: controlling food intake and body weight. J Clin Invest 2014;124(10):4223—6.

[61] Holt MK, Richards JE, Cook DR, Brierley DI, Williams DL, Reimann F, et al. Preproglucagon neurons in the nucleus of the solitary tract are the main source of brain GLP-1, mediate stress-induced hypophagia, and limit unusually large intakes of food. Diabetes 2019;68(1):21—33.

[62] Pyke C, Heller RS, Kirk RK, Orskov C, Reedtz-Runge S, Kaastrup P, et al. GLP-1 receptor localization in monkey and human tissue: novel distribution revealed with extensively validated monoclonal antibody. Endocrinology 2014;155(4):1280—90.

[63] Terrill SJ, Maske CB, Williams DL. Endogenous GLP-1 in lateral septum contributes to stress-induced hypophagia. Physiol Behav 2018;192:17—22.

[64] Imbernon M, Saponaro C, Helms HCC, Duquenne M, Fernandois D, Deligia E, et al. Tanycytes control hypothalamic liraglutide uptake and its anti-obesity actions. Cell Metab 2022;34(7):1054—63. e1057.

[65] Kastin AJ, Akerstrom V. Entry of exendin-4 into brain is rapid but may be limited at high doses. Int J Obes Relat Metab Disord 2003;27(3):313—8.

Original article

[66] Buller S, Blouet C. Brain access of incretins and incretin receptor agonists to their central targets relevant for appetite suppression and weight loss. Am J Physiol Endocrinol Metab 2024;326(4):E472—80.

[67] Rinaman L. Ascending projections from the caudal visceral nucleus of the solitary tract to brain regions involved in food intake and energy expenditure. Brain Res 2010;1350:18—34.

[68] Singh I, Wang L, Xia B, Liu J, Tahiri A, El Ouaamari A, et al. Activation of arcuate nucleus glucagon-like peptide-1 receptor-expressing neurons suppresses food intake. Cell Biosci 2022;12(1):178.

[69] McMorrow HE, Lorch CM, Hayes NW, Fleps SW, Frydman JA, Xia JL, et al. Incretin hormones and pharmacomimetics rapidly inhibit AgRP neuron activity to suppress appetite. bioRxiv 2024. 2024.2003.2018.585583. preprint.